Mottl, M.J., Davis, E.E., Fisher, A.T., and Slack, J.F. (Eds.), 1994
Proceedings of the Ocean Drilling Program, Scientific Results, Vol. 139

48. *DATA REPORT:* SULFUR CONTENT OF SEDIMENT AND SULFUR ISOTOPE VALUES OF SULFIDE AND SULFATE MINERALS FROM MIDDLE VALLEY[1]

Robert A. Zierenberg[2]

INTRODUCTION

Sulfide sulfur content of sediment and sulfur isotope ratios of sulfide and sulfate minerals were measured as part of an effort to determine the sources and mass and isotope fluxes of sulfur in and near the Middle Valley hydrothermal system. Limited access to mass spectrometry facilities resulted in the late attainment of these data relative to the deadline for submission of manuscripts to this volume. Therefore, these data are presented as a data report without significant interpretation.

METHODS

Samples for sulfur isotope analyses were classified by major lithology as sediment, diabase, basalt, massive sulfide, or clastic sulfide redeposited from massive sulfide. Sediment samples were classified as clay, silt, or sand based on a visual estimation of the dominant grain size. Total sulfide sulfur was chemically extracted from bulk samples of unlithified sediment by acid dissolution in 6N HCl using chromous chloride as a reductant (Canfield et al., 1986). H_2S produced in the reaction was stripped from the solution by N_2 gas and precipitated as Ag_2S. The weight of Ag_2S produced relative to the starting weight of sediment provides a measure of the sulfide sulfur content in the sediments (Table 1). Injection of HCl into the reaction vessels prior to addition of $CrCl_2$ allowed detection and separation of acid-volatile sulfide minerals such as pyrrhotite, mackinawite, and greigite. Acid volatile sulfide was detected only in trace amounts and only in a small number of samples. The total sulfide content and the sulfur isotope data therefore reflect pyritic sulfur (Table 1).

In more lithified sediment samples and in samples of basalt, diabase, or massive sulfide, subsamples for sulfur isotope analyses were taken by drilling with diamond-impregnated bits using a handheld dental drill. This often allowed sampling of individual minerals, veins, burrow fills, or nodules of sulfide and sulfate minerals. Separate subsamples are listed on separate lines in Table 1. When more than one mineral was analyzed from the same subsample the results are listed on the same line of the table. Because of the selective sampling, sulfur contents are not reported for these samples. All sulfide samples were chemically treated to extract monosulfide sulfur (sphalerite and/or pyrrhotite), by dissolution under an N_2 atmosphere in 6N HCl, followed by extraction of disulfide sulfur (pyrite, marcasite, and chalcopyrite) using $CrCl_2$ as a reductant. Sulfate-mineral-bearing samples were treated with 0.5 N HCl to dissolve anhydrite and gypsum; the dissolved sulfate was reprecipitated as $BaSO_4$. Samples with barite were first treated to remove anhydrite and gypsum followed by dissolution of barite in concentrated $NaCO_3$ and reprecipitation as $BaSO_4$, as described by Breit et al. (1985).

Sulfur isotope determinations were made on SO_2 produced by combustion of Ag_2S under vacuum using Cu_2O as an oxidant, or combustion of $BaSO_4$ with Cu_2O plus quartz. Measurements were made on a Finnigan Delta mass spectrometer and standardized against Ag_2S standards with values determined by SF_6 by Rees (1978). Present day seawater sulfate determined by this method gives a value of 20.99‰ relative to Canyon Diablo Troilite (CDT) (Rees et al., 1978).

RESULTS

Site 855

Site 855 was rotary cored in an area of low heat flow near a normal fault that bounds the east side of Middle Valley. Sulfur content of sediments recovered at this site are low (0.1 to 0.3 weight percent [wt%]) and do not vary systematically with depth (Davis, Mottl, Fisher, et al., 1992). Only four samples of pyrite in sediment from Hole 855C were analyzed for sulfur isotope values (Table 1). The $\delta^{34}S$ values range from –40.7‰ to –5.4‰ and there is a poorly defined trend to higher values at depth (Fig. 1).

Site 856

Hole 856A

Hole 856A was drilled in the center of a circular hill of uplifted sediment (Bent Hill). Sediment becomes increasingly indurated and is hydrothermally altered at depth in this hole (Davis, Mottl, Fisher, et al., 1992).

An olivine diabase sill was cored in the bottom 3 m of the hole. Sulfur content is generally between 0.1 and 0.3 wt% in the top 20 m of the hole and becomes more variable and tends towards higher values at depth (Davis, Mottl, Fisher, et al., 1992; Table 1). Disseminated pyrite has $\delta^{34}S$ values between –39.8‰ and 17.7‰ (Fig. 2). The data indicate a general trend to higher values at depth.

Hole 856B

Hole 856B was drilled on the south flank of Bent Hill. In addition to the turbiditic and hemipelagic sediment that fills Middle Valley, an olivine diabase sill approximately 5 m thick occurs at 62 mbsf. Hole 856B ended after drilling approximately 1.5 m into an olivine diabase sill at 120 mbsf. The recovered sediment was generally indurated to hydrothermally altered, especially near the basaltic sills. The bottom 18 m above the basaltic sill is a zone of hydrothermal alteration and sulfide mineralization that becomes more prominent toward the contact. Pyrite is the dominant sulfide mineral through most of the sediment section, but pyrrhotite, sphalerite, and chalcopyrite occur in the mineralized zone adjacent to the sill. Disseminations and veins of anhydrite and barite occur in this interval.

Pyrite is visibly more abundant in Hole 856B than in Hole 856A. Sulfur content of the sediment is typically between 1 and 1.5 wt% (Davis, Mottl, Fisher, et al., 1992). An interval between 18 and 24 mbsf has much higher sulfur content due to the presence of turbidites and debris flows derived from massive sulfide. The $\delta^{34}S$ values of disseminated pyrite in the sediment range from –22.8‰ to 31.3‰ (Table 1). Sulfur isotope values tend to become higher downhole at least to the depth of the first olivine diabase sill (Fig. 3). Below this depth sulfur isotope values of pyrite are fairly constant but range from 6.0‰ to 13.1‰. Sulfur isotope values for the interval containing clas-

[1] Mottl, M.J., Davis, E.E., Fisher, A.T., and Slack, J.F. (Eds.), 1994. *Proc. ODP, Sci. Results*, 139: College Station, TX (Ocean Drilling Program).

[2] U.S. Geological Survey, 345 Middlefield Rd., M.S. 901, Menlo Park, CA 94025-3591, U.S.A.

Table 1. Sulfur content and sulfur isotope values of Middle Valley samples.

				$\delta^{34}S$					
Core, section, interval (cm)	Depth (mbsf)	Lithology	S (%)	Py	Po	Sl	An	Ba	Notes
139-855C-									
2R-4, 139–143	14.59	Silt	0.75	–26.6					
4R-4, 91–93	32.51	Clay	1.84	–40.7					
10R-4, 62–64	88.52	Sand	1.71	–5.4					
11R-1, 101–106	95.61	Sand	0.70	–14.2					
139-856A-									
2H-3, 76–78	6.46	Clay	0.95	–39.8					
3H-3, 30–32	15.50	Silt	4.82	–22.6					
3H-3, 142–146	16.62	Sand	0.32	–18.8					
4H-1, 47–49	22.17	Clay	1.17	–20.3					
4H-1, 95–97	22.65	Clay	0.16						
4H-2, 147–149	24.67	Clay	0.11	–4.7					
4H-3, 32–34	25.02	Clay	0.79	–24.8					
4H-4, 53–55	26.73	Clay	0.04						
4H-6, 80–82	30.00	Sand	0.09	–8.9					
5H-7, 103–105	40.11	Sand	0.43	–4.9					
5H-8, 13–15	40.71	Silt	0.15	–21.0					
5H-8, 86–88	41.44	Clay	4.95	2.4					
6H-3, 65–67	44.35	Sand	0.91	3.8					
6H-4, 64–66	45.84	Silt	0.27	7.4					
6H-6, 1–3	48.21	Silt	0.28						
6H-6, 140–142	49.60	Silt	0.12	–18.1					
7H-1, 127–129	51.47	Silt	1.55	6.8					
7H-5, 3–5	56.23	Clay	0.18	–22.4					
8H-2, 131–133	62.51	Silt	0.31	7.1					
8H-CC, 28–30	69.69	Silt	2.59	–7.8					
10X-1, 131–133	80.01	Clay	0.07						
11X-1, 32–34	86.52	Silt	1.57	–11.5					
12X-1, 139–141	97.09	Silt	0.69	17.7					
13X-1, 111–113	106.41	Silt	0.45	16.2					
13X-3, 68–70	108.98	Silt	0.15	10.5					
139-856B-									
2H-2, 53–56	3.83	Silt	0.65	–22.8					
2H-2, 53–56	3.83	Silt		–17.3					
2H-3, 25–29	5.05	Sand	0.15	–10.4					
2H-5, 8–12	7.88	Clay	1.34	–5.6					
3H-2, 87–89	13.67	Silt	0.35	–2.2					
3H-5, 137–139	18.67	CS		2.1					
3H-6, 51–53	19.31	CS		3.0					
3H-6, 51–53	19.31	CS		3.1					
3H-6, 105–107	19.85	CS		4.7					
3H-6, 105–107	19.85	CS		4.4					
4H-2, 25–27	22.55	CS		–1.1					Total sulfide
4H-2, 25–27	22.55	CS		–1.2					Fresh Py
4H-2, 25–27	22.55	CS		2.3					Weathered Py
4H-5, 77–79	27.57	Silt	9.82	–8.1					
5H-5, 8–11	36.38	Silt	1.05	6.0					
6H-2, 82–85	42.12	Clay	0.58	–7.0					
6H-2, 134–136	42.64	Clay	0.22	3.7					
6H-4, 117–119	45.47	Clay	0.60	8.0					
7H-1, 25–28	49.55	Silt	0.32	3.2					
7H-3, 89–92	53.19	Silt		8.8					Total sulfide
7H-3, 89–92	53.19	Silt		9.5					Py nodule
7H-3, 89–92	53.19	Silt		10.4					Py nodule
7H-3, 89–92	53.19	Silt					10.1		
7H-3, 89–92	53.19	Silt					4.2		
7H-4, 67–70	54.47	Silt		–0.8					Total sulfide
7H-4, 67–70	54.47	Silt	0.94	–16.8					Py filled burrow
7H-6, 44–47	57.24	Clay	6.2 2	31.3					
8H-4, 42–44	63.60	Clay	1.28	7.9					
9X-1, 20–22	63.86	Silt	1.32	4.3					
11X-5, 42–45	79.72	Silt	1.38	12.7					
12X-5, 71–73	88.31	Silt	5.01	7.7					
12X-5, 107–109	88.67	Clay	0.38	11.4					
12X-5, 117–119	88.77	Clay	0.39	10.1					
12X-5, 117–119	88.77	Clay		8.8					
13X-1, 112–114	92.22	Clay	3.17	13.1					
13X-2, 79–83	93.39	Clay	0.25	10.8					
14X-4, 24–31	105.54	Clay		9.5					Total sulfide
14X-4, 24–31	105.54	Clay		7.2		10.2			Co-existing Py-Sl
14X-4, 50–55	105.80	Clay		10.3					
14X-CC, 34–38	106.51	Sand		7.2					
15X-1, 27–29	110.67	Clay		6.6					
15X-1, 65–67	111.05	Clay		6.2					
15X-1, 137–139	111.77	Clay		7.1					
15X-3, 42–44	113.82	Clay		7.3					
15X-3, 108–110	114.48	Clay		6.7				22.7	
15X-4, 107–109	115.97	Clay						21.8	
15X-4, 128–130	116.18	Clay		6.5				23.9	
15X-5, 34–36	116.74	Clay		7.3		6.9	21.6		
15X-5, 119–121	117.59	Silt					23.2		
15X-CC, 12–14	118.14	Clay		6.0				23.8	Py-Ba vein
16X-1, 17–19	120.27	Clay		6.0		6.0		22.2	Py-Ba vein

Table 1 (continued).

Core, section, interval (cm)	Depth (mbsf)	Lithology	S (%)	$\delta^{34}S$					Notes
				Py	Po	Sl	An	Ba	
139-856D-									
1H-1, 43–44	0.43	MS		4.6					
1H-1, 43–44	0.43	MS		5.3					
1H-3, 140–150	4.40	MS		6.7					
1H-3, 140–150	4.40	MS		4.7					
1H-4, 34–35	4.84	MS		4.5					
1H-4, 79–82	5.29	MS		4.7					
1H-5, 14–15	6.14	MS		4.5					
1H-5, 14–15	6.14	MS		4.6					
1H-7, 78–80	8.21	MS		5.0					
1H-7, 78–80	8.21	MS		5.8					
1H-7, 78–80	8.21	MS		12.3		7.5			
139-856G-									
3R-1, 7–8	17.67	MS		5.2					
3R-1, 7–8	17.67	MS		5.7					
4R-1, 131–133	28.31	MS		8.1					
5R-1, 44–46	37.14	MS		6.3					
6R-1, 36–38	46.66	MS		7.5					
6R-1, 36–38	46.66	MS				3.1			Sl vein
6R-2, 140–142	49.20	MS		8.3	8.3				
6R-2, 140–142	49.20	MS		6.2					
6R-3, 24–26	49.54	MS		8.3					
6R-3, 79–81	50.09	MS		8.9					
6R-3, 79–81	50.09	MS		12.4					
7R-2, 27–29	57.47	MS		9.7					
7R-2, 27–29	57.47	MS		4.9					
7R-3, 98–100	59.67	MS		8.5					
7R-3, 98–100	59.67	MS		7.7					
7R-4, 4–6	60.14	MS		8.0		5.5			
139-856H-									
1R-CC, 7–9	4.00	MS		6.0					
1R-CC, 7–9	4.00	MS		5.7					
3R-1, 78–80	22.88	MS		4.4					
3R-1, 78–80	22.88	MS		3.8					
3R-2, 45–47	23.71	MS		5.7					
3R-3, 24–26	24.95	MS		7.8		8.3			
4R-1, 48–50	27.08	MS		6.7					
4R-1, 48–50	27.08	MS		5.8					
4R-1, 142–144	28.02	MS		5.9	7.6				
4R-1, 142–144	28.02	MS		7.9					Coarse Py
4R-1, 142–144	28.02	MS				8.2			Course Sl
4R-2, 12–14	28.22	MS		7.5					
4R-2, 50–52	28.60	MS		7.1	7.3				Po clast
4R-2, 50–52	28.60	MS		8.2					
5R-1, 27–28	32.67	MS		8.1	7.8				
6R-1, 12–14	37.52	MS		6.4					
6R-1, 12–14	37.52	MS		6.3					
8R-1, 30–32	48.30	MS		5.3					
8R-1, 30–32	48.30	MS		5.0					
8R-1, 115–117	49.15	MS		6.7				20.9	
9R-1, 7–9	52.57	MS		7.0					
10R-1, 50–51	57.50	MS		2.6					
11R-1, 107–109	62.37	MS		1.9					
13R-1, 2–4	70.92	MS		6.7					
14R-1, 132–134	77.02	MS			5.0				
14R-1, 132–134	77.02	MS		6.9	6.4				
14R-1, 132–134	77.02	MS		5.6					Py porphyroblast
14R-1, 132–134	77.02	MS		–8.0					Late vug filling Py
15R-1, 127–129	81.77	MS		7.5					
16R-1, 4–6	85.24	MS		4.9	5.0				
16R-1, 4–6	85.24	MS		–1.9					Late vug filling Py
16R-1, 31–32	85.51	MS		5.0					
17R-1, 33–34	90.43	MS		6.7	6.7				
17R-1, 33–34	90.43	MS		2.5					Chalcopyrite
139-857A-									
4H-3, 119–121	26.09	Clay	1.85	–30.3					
5H-4, 81–83	36.71	Clay	4.63	–21.7					
6H-2, 102–106	43.42	Silt	0.20	–8.0					
8H-3, 117–119	64.07	Silt	0.30	0.6					
8H-3, 117–119	64.07	Silt		3.1					Py nodule
10H-2, 123–125	81.63	Silt	1.54	9.0					
13X-1, 117–119	102.67	Silt	0.83	11.9					
139-857C-									
2R-1, 28–31	56.78	Silt	1.33	–12.0					
2R-1, 28–31	56.78	Silt					–11.2		
2R-1, 28–31	56.78	Silt					–6.6		
3R-2, 106–108	69.06	Silt	0.14	–16. 7					
13R-1, 62–64	153.72	Sand	3.41	2.0					
14R-1, 47–51	163.27	Clay	0.41	6.6					
15R-1, 1–3	172.51	Sand	0.09	17.2					
15R-1, 61–63	173.11	Silt	0.26	18.0					
17R-2, 84–88	194.24	Silt	0.09	–8.4					
22R-1, 144–147	241.74	Clay	0.14	–0.5					
30R-2, 147–150	316.07	Silt	0.03	10.5					
31R-3, 14–16	325.84	Silt	0.10	–2.2					

Table 1 (continued).

Core, section, interval (cm)	Depth (mbsf)	Lithology	S (%)	δ³⁴S Py	Po	Sl	An	Ba	Notes
31R-CC, 0–3	326.02	Clay	0.49	1.5					
33R-1, 100–102	333.40	Silt	0.21	6.4					
33R-1, 123–125	333.63	Silt	0.27	9.1					
33R-2, 133–135	335.23	Clay	0.29	6.8					
34R-3, 37–39	339.87	Silt	0.26	−1.6					
34R-3, 67–70	340.17	Clay	0.23	−25.4					
35R-1, 66–68	341.96	Silt	0.12	−26.5					
35R-2, 44–46	343.24	Clay		−12.0					
37R-2, 121–123	353.51	Clay		−11.3					
38R-1, 4–6	355.84	Clay		−9.6					Burrow fill py
39R-1, 119–121	361.59	Clay		38.8					
41R-1, 144–146	376.34	Clay		−1.2					
42R-2, 29–31	381.49	Silt		15.0					
43R-3, 0–4	387.70	Sand		54.3					MS clasts in turbidite
49R-1, 111–114	414.81	Clay		29.1					
50R-2, 58–60	420.38	Clay		16.8					Py vein
50R-2, 75–77	420.55	Clay		15.3					Py nodule
51R-2, 18–20	425.08	Sand		13.6					
56R-1, 0–2	446.50	Clay		12.4					Py vein
57R-1, 11–12	451.81	Sand		14.3					Coarse euhedral Py
58R-1, 2–3	461.52	Clay		12.8					Py vein
59R-1, 3–4	471.13	Diabase		9.3					Py-Chl vein
59R-1, 3–4	471.13	Diabase				7.6			Sl-Cp-Wai vein
59R-4, 72–74	476.24	Diabase		−0.2					Chl-Py selvage of Epi vein
60R-1, 126–128	482.06	Diabase		8.0					
61R-1, 41–43	490.91	Diabase		8 .4					
62R-1, 120–130	501.20	Diabase		3.6					
63R-1, 29–31	509.99	Silt		13.6					
64R-2, 57–59	521.47	Diabase				7.5			Wai-Sl vein
65R-1, 2–4	529.12	Diabase		7.5					
66R-1, 2–3	538.82	Sand		15.5					
68R-1, 8–10	558.08	Diabase		5.2					
139-857D-									
1R-1, 42–44	581.92	Diabase				7.7			Sl-Cp Wai vein
3R-1, 62–63	599.92	Diabase		8.4					Selvage of Epi-Qtz-Py-Cp vein
4R-1, 133–136	610.23	Diabase		8.1					
5R-1, 16–18	618.76	Sand		9.6	8.3				
6R-1, 2–4	627.92	Silt			8.7				Qtz Po vein
8R-1, 31–33	647.61	Diabase		9.4					Py-Chl vein in quenched margin
9R-1, 25–27	657.15	Diabase		9.3					Py Wai? vein
12R-1, 75–77	686.65	Diabase			8.2				Po-Wai-Qtz vein
12R-1, 121–124	687.11	Diabase		8.5					Wai-Qtz-Py vein
15R-1, 55–57	715.35	Diabase		10.2					
16R-1, 48–50	724.98	Silt		13.0					
17R-1, 96–98	734.86	Silt		14.6					
18R-1, 94–96	744.54	Diabase		7.2					
22R-1, 45–46	782.25	Diabase		11.1					Py-Epi vein
24R-1, 100–102	802.20	Clay		11.4					Py vein
24R-2, 45–47	803.15	Diabase		12.0					
26R-1, 39–41	820.69	Diabase		10.0					
27R-1, 22–24	829.22	Diabase		9.9		8.6			Qtz-Wai-Epi-Sl-Py vein
28R-1, 50–52	839.40	Silt		9.0					
29R-2, 40–42	850.30	Diabase		11.2					
31R-1, 20–24	868.70	Sand		10.9					
33R-1, 92–93	888.72	Diabase		7.9					Epi-Py vein
36R-1, 129–131	918.19	Diabase		7.7					
139-858A-									
2H-7, 34–38	11.74	Clay	0.60	3.4					
3H-1, 87–91	12.77	Silt	0.71	−5.6					
5H-5, 65–68	37.55	Silt	0.19	7.6					
6H-3, 144–146	44.84	Silt	1.50	−2.3					
6H-CC, 7–9	44.97	Clay	1.73	−5.3					
7H-4, 105–108	55.46	Silt	0.79	16.0					
9X-2, 136–138	65.36	Silt	0.04	5.9					
9X-3, 10–12	65.60	Clay	1.27	25.6			24.2		An-Gyp cement
9X-3, 10–12	65.60	Clay		9.8					Coarse Py
9X-3, 61–63	66.11	Clay	0.22	11.2					
9X-5, 96–98	69.46	Clay	0.56	−21.0					
11X-CC, 7–8	73.54	Clay	1.20	1.3					
12X-CC, 5–6	81.85	Sand		22.3					
14X-CC, 3–5	101.03	Sand		−9.7					
17X-CC, 2–5	130.27	Clay					21.3		Dissm bladed An
18X-1, 6–8	139.66	Sand					26.3		
18X-2, 127–130	142.37	Silt		28.9			25.0		
18X-CC, 6–8	143.04	Clay					21.9		
19X-1, 43–45	149.73	Silt					28.3		
20X-3, 135–138	163.28	Clay		25.0					An-Gyp vein
20X-4, 15–18	163.59	Clay		27.0					
21X-1, 67–70	169.27	Sand		14.3			26.4		
21X-2, 28–31	170.38	Clay					25.0		An-Gyp vein
21X-2, 71–74	170.81	Silt		1.9			22.4		
22X-1, 10–11	178.30	Clay		12.0			27.4		Dissm bladed An
23X-1, 71–73	188.61	Clay		14.2					
24X-1, 61–63	198.21	Silt		−32.4					
26X-CC, 6–8	216.96	Clay	0.37	7.7			25.8		

Table 1 (continued).

Core, section, interval (cm)	Depth (mbsf)	Lithology	S (%)	δ34S Py	Po	Sl	An	Ba	Notes
29X-1, 7–11	245.97	Sand		8.3					
30X-1, 41–44	256.01	Clay		8.2					
31X-1, 26–28	265.56	Clay		9.3					Coarse Py cubes
38X-CC, 10–12	322.80	Sand		9.2					
139-858B-									
1H-2, 27–29	1.77	Clay	0.49	−0.5					
1H-5, 3–5	6.03	Silt	0.54	−13.7					
1H-CC, 20–22	7.10	Clay		−15.3				44.6	
2H-3, 27–29	10.47	Clay		4.5					Semi-MS
2H-3, 119–121	11.39	Clay		4.1			26.3		Semi-MS
2H-4, 7–9	11.77	Clay		1.7			23.7		Semi-MS
139-858C-									
3H-2, 101–104	15.51	Clay		8.5			5.9		
3H-3, 133–135	17.33	Clay		15.2			14.7		
5H-1, 139–141	24.98	Silt		−2.4					
5H-5, 27–29	29.77	Silt		−2.8			3.0		Gyp
6H-1, 143–145	34.43	Silt		3.6			22.6		
6H-3, 82–83	36.82	Clay		1.8			22.3		An vein
7H- 1, 32–34	41.82	Clay		4.3			22.5		
7H-2, 138–141	44.38	Clay		−0.4					
8H-1, 58–59	47.08	Silt		−3.4			22.7		Coarse Py, An nodule
10X-CC, 6–9	49.56	Silt		1.5					
11X-CC, 30–32	55.78	Silt		9.0					
12X-1, 18–20	64.18	Silt		4.8					
13X-1, 2–5	73.72	Silt		8.3					
13X-1, 41–46	74.14	Clay		8.0			23.8		
14X-CC, 28–30	84.46	Silt		−9.2			12.3		
139-858D-									
2H-4, 10–13	13.90	Clay		15.1					
4H-3, 138–140	22.92	Clay		−18.7			23.5		
4H-4, 56–58	23.60	Silt		4.9			23.2		
6X-1, 61–64	29.41	Clay		6.6					
139-858F-									
11R-CC, 12–14	114.09	Sand					23.4		
13R-CC, 0–2	132.90	Clay		14.7					
13R-CC, 15–17	133.05	Sand		12.1					
14R-1, 16–17	142.76	Silt		11.6					
15R-CC, 1–2	152.21	Silt					22.2		
19R -1, 26–27	191.16	Silt		11.5					
19R-1, 37–38	191.27	Sand		11.1					
21R-1, 14–16	210.44	Clay		11.0			11.4		
21R-1, 14–16	210.44	Clay		12.7					
22R-CC, 12–13	220.12	Silt		9.3					
23R-CC, 6–7	229.66	Clay		6.3					
24R-CC, 8–10	239.38	Clay		−12.6					
24R-CC, 8–10	239.38	Clay		−13.2					
25R-1, 36–37	249.26	Silt		11.1					
25R-1, 36–37	249.26	Silt		11.4					
25R-1, 75–76	249.65	Silt		12.5					
25R-1, 107–108	249.97	Basalt		13.3					Qtz-Wai-Py vein
25R-1, 111–112	250.01	Basalt		13.8					Qtz-Wai-Py vein
28R-1, 19–20	277.69	Basalt		4.0					
139-858G-									
2R-1, 65–67	287.15	Basalt		5.8					Py-Chi vein
4H-1, 23–25	306.03	Basalt					22.5		An vein
5R-1, 1–3	315.41	Basalt			10.3				
6R- 1, 29–31	325.39	Basalt		8.1					Py-Chl vein
10R-1, 43–45	365.33	Basalt		9.7					
13R-1, 45–47	394.35	Basalt		8.8					
16R-1, 88–89	423.78	Basalt		7.3					

Notes: MS = massive sulfide, CS = clastic sulfide, Py = pyrite, Po = pyrrhotite, Sl = sphalerite, Cp = chalcopyrite, An = anhydrite, Gyp = gypsum, Ba = barite, Qtz = quartz, Chl = chlorite, Wai = wairakite, Epi = epidote, Dissm = disseminated.

ticly deposited massive sulfide have a narrow range from −1.2‰ to 4.7‰. Sphalerite was separated from three samples of the mineralized zone at the base of the hole. Sphalerite $\delta^{34}S$ values range from 6.0‰ to 10.2‰ and are not in isotopic equilibrium with coexisting pyrite. Disseminated anhydrite and barite from this interval are slightly enriched in ^{34}S relative to seawater sulfate and range in value from 21.6‰ to 23.9‰; barite in veins gave values of 22.2‰ and 23.8‰. Two samples of disseminated sulfate (probably gypsum) in silt from 53.19 mbsf have values of 10.1‰ and 4.2‰, consistent with derivation of sulfate by local oxidation of pyrite from this interval (Table 1).

Hole 856D

Hole 856D was piston cored into the weathered, rubbly top of a ridge of massive sulfide that occurs on the south flank of Bent Hill. Recovered material was disaggregated and partly weathered massive sulfide composed predominately of sand- to silt-sized pyrite grains and aggregates, with less abundant amorphous silica, sphalerite, pyrrhotite, and chalcopyrite. Pyrite from this core has $\delta^{34}S$ values of 4.6‰ to 5.7‰ except for one sample fragment from near the base of the core at 8.21 mbsf that yields values of 12.3‰ and 7.5‰ for coex-

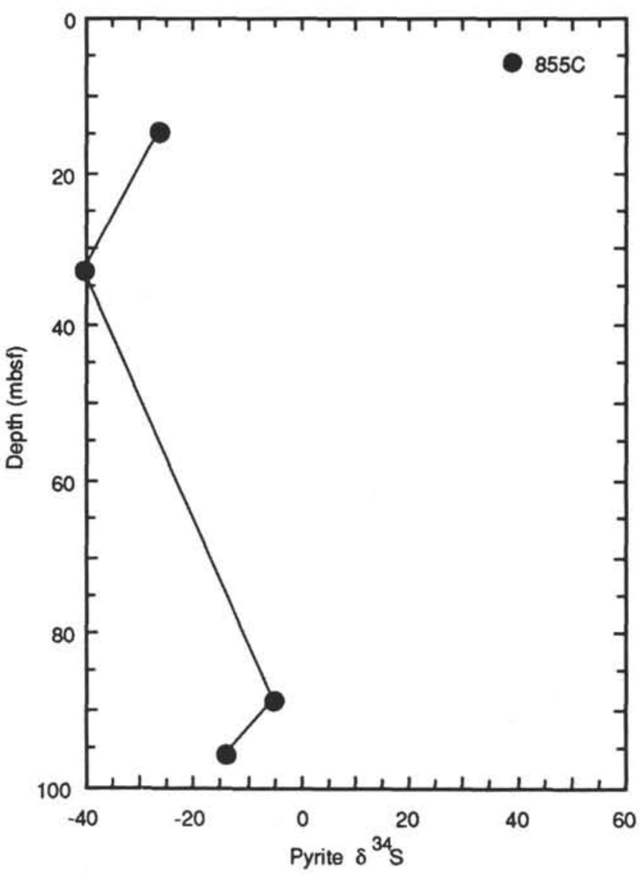

Figure 1. Sulfur isotope value of pyrite vs. depth for Hole 855C.

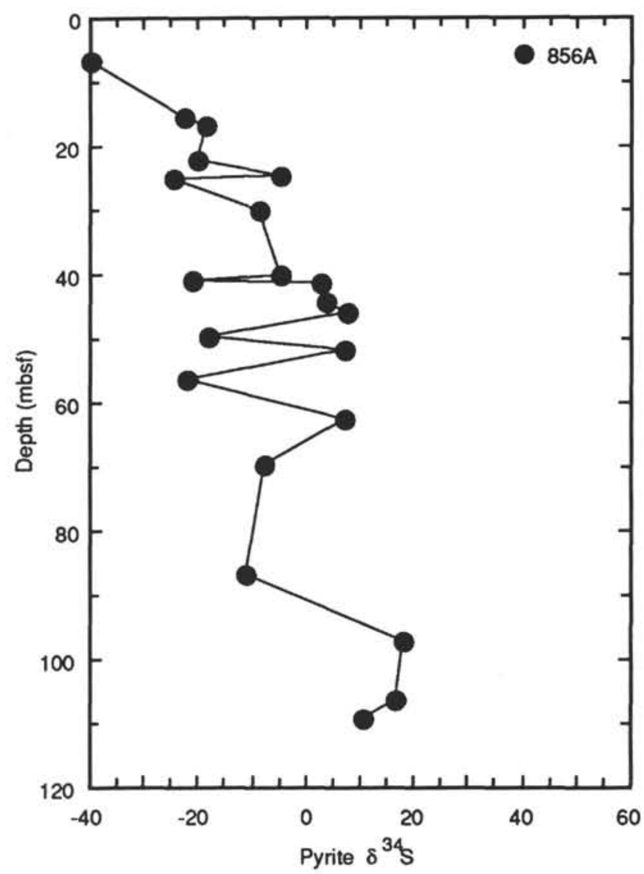

Figure 2. Sulfur isotope value of pyrite vs. depth for Hole 856A.

isting pyrite and sphalerite, respectively. These values are not consistent with isotopic equilibrium between the two sulfide minerals.

Hole 856G

Hole 856G was rotary cored near the top of the ridge of massive sulfide on the south flank of Bent Hill. This hole penetrated 65.4 m of massive sulfide before the hole was abandoned due to adverse drilling conditions. Massive sulfide recovered in this hole is described in Davis, Mottl, Fisher, et al. (1992). Pyrite from Hole 856G ranges in $\delta^{34}S$ value from 4.9‰ to 12.4‰, but most values are between 5‰ and 9‰ (Fig. 4). Coexisting pyrrhotite and pyrite from Sample 139-856G-6R-2, 140–142 cm have identical values of 8.3‰, which is indicative of nonequilibrium but is consistent with pyrite inheriting pyrrhotite sulfur during replacement. Coexisting pyrite and sphalerite in Sample 139-856G-7R-4, 4–6 cm have values of 8.0‰ and 5.5‰, respectively, which are also incompatible with isotopic equilibrium at temperatures above 0°C. A late-stage sphalerite vein in Sample 139-856G-6R-1, 36–38 cm has a value of 3.1‰, which is 4.4‰ lighter than pyrite in the wall rock. The sulfur isotope values of massive sulfide in Hole 856G do not vary systematically between the different sulfide types defined in Davis, Mottl, Fisher, et al. (1992).

Hole 856H

Hole 856H was rotary cored near the top of the ridge of massive sulfide on the south flank of Bent Hill adjacent to Hole 856G. This hole penetrated 93.8 m of massive sulfide before the hole was abandoned due to adverse drilling conditions. Massive sulfide recovered in this hole is described in Davis, Mottl, Fisher, et al. (1992). Pyrite from Hole 856H ranges in $\delta^{34}S$ value from –8.0‰ to 8.2‰, but most values are between 5‰ and 9‰, similar to samples from Hole 856G (Fig. 5). Two samples of paragenetically late, vug-filling pyrite have negative sulfur isotope values (–1.9‰ and –8.0‰). Pyrrhotite values range from 5.0‰ to 7.8‰. With one exception, coexisting pyrite and pyrrhotite have $\delta^{34}S$ values that are within 0.5‰; in Sample 139-856H-4R-1, 142–144 the pyrrhotite value is within 0.3‰ of coarse-grained pyrite "porphyroblasts" that replace pyrrhotite. However, none of the sample pairs appear to represent isotopic equilibrium. They are consistent with pyrite forming by replacement of pyrrhotite through a process that conserves sulfur, as is suggested by petrographic observations. Two microdrilled samples of sphalerite give values of 8.2‰ and 8.3‰, near the upper range of values for pyrite in this hole. One sample of chalcopyrite has a relatively low sulfur isotope value of 2.5‰. One barite sample gives a value of 20.9‰, identical to seawater sulfate. As in Hole 856G, sulfur isotope values of massive sulfide in 856H do not vary systematically with sulfide type.

Site 857

Site 857 was drilled in an area of relatively high heat flow (700–800 mW) about 1.6 km south of the large hydrothermal vent field at Site 858. Samples for sulfur isotope analyses were collected from Holes 857A, 857C, and 857D. Hole 857A was drilled by advanced piston core–extended core barrel (APC-XCB) to 112 m depth. Holes 857C and 857D were drilled about 200 m east of Hole 857A and were rotary cored. At both Holes 857C and 857D, interlayered diabase sills and metasedimentary rock were encountered at depths greater than 460 m. Hole 857D was the deepest penetration in the Middle Valley area with a total depth of 936.2 m.

Hole 857A

Core recovered from Hole 857A consisted of interbedded turbiditic and hemipelagic sediment. Pore-water sulfate in Hole 857A de-

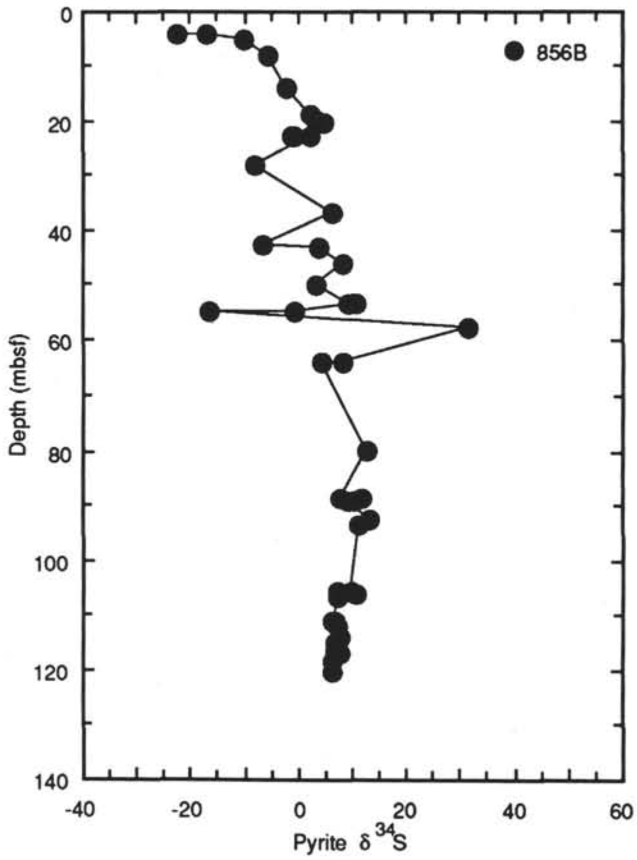

Figure 3. Sulfur isotope value of pyrite vs. depth for Hole 856B.

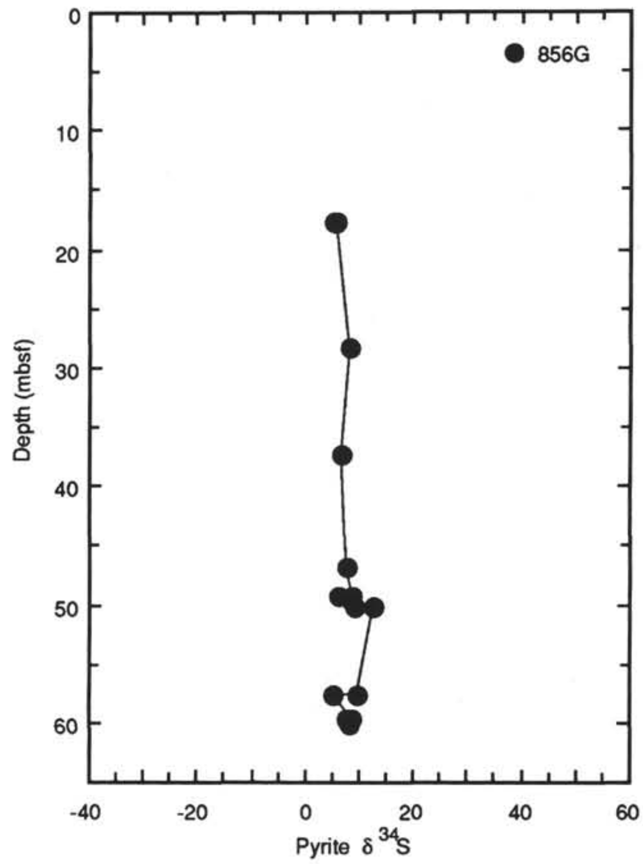

Figure 4. Sulfur isotope value of pyrite vs. depth for Hole 856G.

creases downhole to about two-thirds of bottom-water values due to bacterial reduction of sulfate (Davis, Mottl, Fisher, et al., 1992). Sulfur content of sediment is generally less than 0.5 wt% (Davis, Mottl, Fisher, et al., 1992). Sulfur isotope values of pyrite in sediment increase from –30.3‰ at 26 mbsf to 11.9‰ at 103 mbsf (Fig. 6). A pyrite nodule at 64 m depth is 2.5‰ higher than disseminated pyrite in the sediment.

Hole 857C

Turbiditic and hemipelagic sediment in Hole 857C becomes increasingly lithified with depth. Basaltic sills are interbedded with metasedimentary rock below 471 m. Pore-water sulfate values decrease downhole to a depth of about 200 mbsf, below which sulfate content is relatively constant at approximately 5 mmol/kg (Davis, Mottl, Fisher, et al., 1992). Sulfur content of the sediment is generally less than 0.5‰. Pyrite $\delta^{34}S$ values in Hole 857C have a wide range of values, from –26.5‰ to 54.3‰ (Fig. 6). Pyrite $\delta^{34}S$ values in sediment are similar to those in Holes 856A, 856B, and 857A in that they generally increase with depth and show less variation with depth, approaching a value near 13‰. Pyrite burrow fills, veins, and nodules all have values similar to disseminated pyrite in nearby sediment. The extreme value of 54.3‰ is from the base of a coarse sand turbidite at 387.7 mbsf that contains clasts of massive sulfide composed of pyrite, pyrrhotite, and sphalerite (Davis, Mottl, Fisher, et al., 1992). These clasts of massive sulfide are the only evidence of a much earlier phase of hydrothermal activity in Middle Valley. This extremely heavy sulfur isotope value is uncommon in seafloor hydrothermal systems.

Two samples of sulfate from 56.78 mbsf were analyzed. A leak in the vacuum extraction line occurred during conversion of the sample, yielding a value of –6.6‰. This leak was partially fixed before the sample conversion was repeated, yielding a value of –11.2‰. This lighter value is considered to be more reliable and is close to the value of pyrite in the same sediment interval (–12.0‰). The sulfate analyzed is probably gypsum which formed by oxidation of pyrite. Pyrite in diabase from Hole 857C ranges in value from –0.2‰ to 9.3‰. Petrographic observations indicate that all of the pyrite in the diabase is of hydrothermal origin and is not magmatic sulfide (Stakes and Franklin, this volume). The value of –0.2‰ is from the chlorite-pyrite selvage of an epidote vein cutting diabase and the value of 9.3% is from a pyrite chlorite vein in diabase. Two samples of sphalerite from wairakite-bearing veins in diabase have values of 7.5‰ and 7.6‰. Pyrite in sediment from the section intruded by the diabase sills tends to be several per mil heavier than pyrite in the diabase.

Hole 857D

Pyrite sampled from Hole 857D includes hydrothermal pyrite in diabase sills and pyrite in sediment between diabase sills. Pyrite in sediment ranges in $\delta^{34}S$ value from 9.0‰ to 14.6‰ and is generally heavier than pyrite in adjacent diabase sills (Fig. 6). One sample of pyrrhotite in sediment has a value of 8.3‰, 1.3‰ lighter than coexisting pyrite. The temperature calculated by assuming isotopic equilibrium between the pair is 110°C, suggesting that the assumption of equilibrium is not valid, as it is below the present temperature at this depth. Pyrrhotite from a quartz-pyrrhotite vein has a value of 8.7‰. Pyrite in diabase sills ranges from 7.2‰ to 12.0‰. Pyrite in veins cutting diabase falls within this range. Pyrrhotite from a wairakite-quartz vein cutting diabase has a value of 8.2‰; sphalerite from wairakite-bearing veins gives values of 7.7‰ and 8.6‰.

Site 858

Drilling at Site 858 consisted of a transect of holes from the margin to the center of an active hydrothermal field. Approximately 20 active

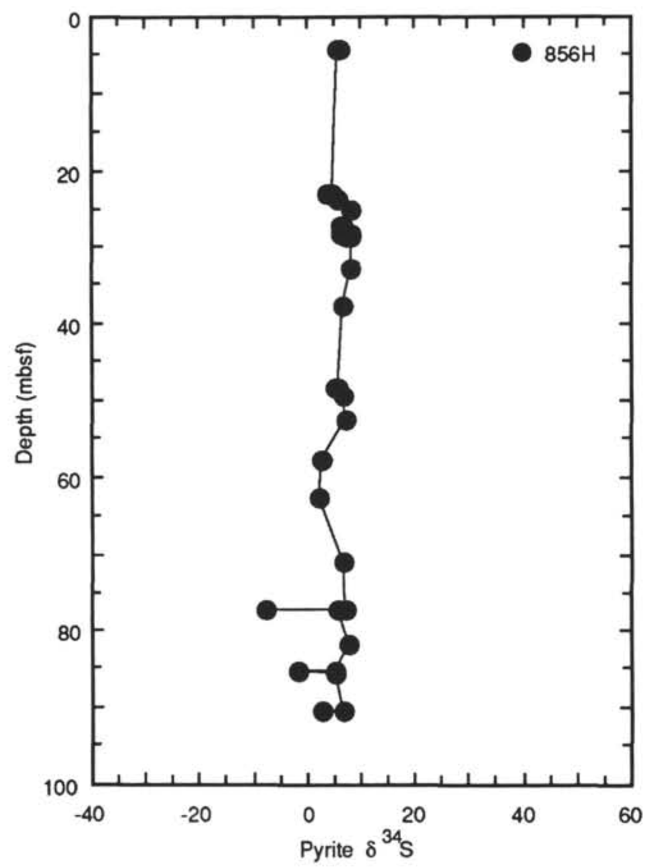

Figure 5. Sulfur isotope value of pyrite vs. depth for Hole 856H.

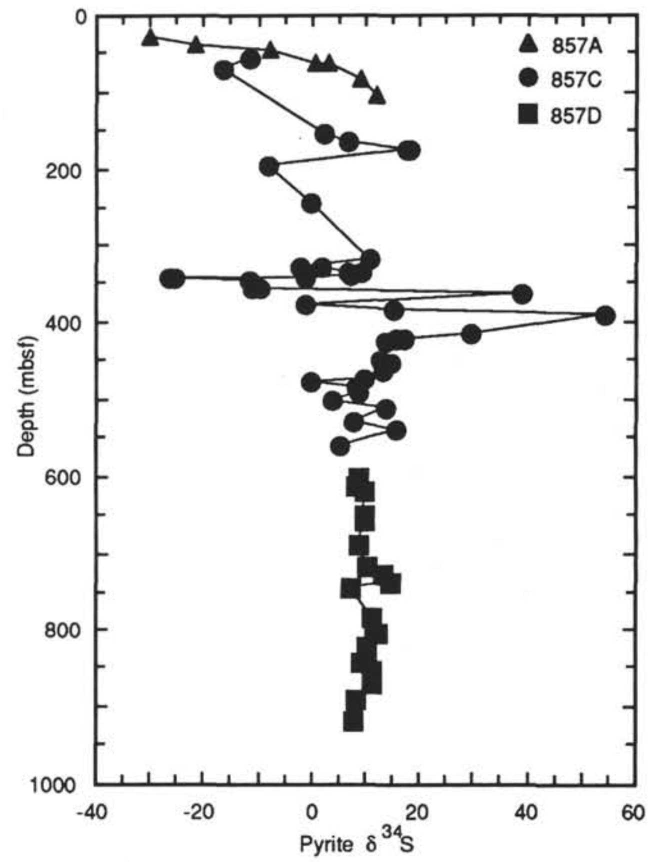

Figure 6. Sulfur isotope value of pyrite vs. depth for Holes 857A, 857C, and 857D.

hydrothermal vents have been mapped in this area. Hydrothermal fluid at temperatures up to 276°C vents from anhydrite chimneys which contain only minor amounts of sulfide (Davis, Mottl, Fisher, et al., 1992). Pore-water sulfate profiles in all of the Site 858 holes cannot be interpreted simply in terms of bacterial sulfate reduction because the high temperature of the sediment has resulted in precipitation anhydrite, some of which can redissolve during core retrieval and processing (Davis, Mottl, Fisher, et al., 1992). Similarly, sulfur contents of sediments from Site 858 reported in Davis, Mottl, Fisher, et al. (1992) cannot be interpreted in terms of pyrite content because of the presence of abundant anhydrite in many sediment samples. Percent sulfur reported in Table 1 of this report does represent the sulfide-sulfur, and not sulfate-sulfur, content of the sediment samples.

Hole 858A

Hole 858A is located about 200 m west of the center of the active vent field and was APC-XCB cored to a depth 339.1 m in turbiditic and hemipelagic sediment and metasediment. Pyrite $\delta^{34}S$ values range from –32.4‰ to 28.9‰ (Fig. 7). A downhole increase in $\delta^{34}S$ values is not as readily apparent in Hole 858A as in holes further from the hydrothermal center. However, samples from below 200 mbsf do have relatively constant sulfur isotope values near 9‰, similar to deep samples from other Middle Valley sites. Anhydrite and gypsum that occur disseminated in sediment, cementing sediment, or as veins have $\delta^{34}S$ values of 21.3‰ to 28.3‰. The lowest values are near the value of seawater sulfate, but most samples are enriched in ^{34}S by several per mil.

Hole 858B

Hole 858B was hydraulically piston cored 20 m away from an active hydrothermal vent. Sediment recovered from this short hole was highly altered by magnesium metasomatism and contained abundant pyrite and anhydrite, including an interval containing semimassive sulfide at approximately 10–12 mbsf. Pyrite $\delta^{34}S$ values range from –15.3‰ to 4.5‰ (Fig. 8). Samples of semimassive sulfide have values of 1.7‰ to 4.5‰. Anhydrite in the altered sediment has values of 23.7‰ and 26.3‰. One sample of barite is highly enriched in ^{34}S with a value of 44.6‰.

Hole 858C

Hole 858C was APC-XCB cored to a depth of 93.1 m. This hole is located within 200 m of both Hole 858A and Hole 858B and is approximately 100 m away from the Dead Dog mound hydrothermal vents. Pyrite in sediment from this hole has $\delta^{34}S$ values of –9.2‰ to 15.2‰ (Fig. 8). Pyrite sulfur isotope values are less variable downhole than in Hole 858A. The deepest samples have values near 8‰ except for the sample from near the bottom of the hole at 84.46 mbsf, which has the lowest value in the hole (–9.2‰). Anhydrite from the middle section of this hole has values between 22.3‰ and 23.8‰, similar to those in Hole 858A. However, three samples from the top 30 m of the hole and the deepest sample in the hole have values below that of seawater sulfate and require input of a lighter source of sulfur, such as H_2S or pyrite that has been oxidized to sulfate.

Holes 858D, 858G, and 858F

Holes 858D, 858G, and 858F were drilled in the center of the heat flow anomaly that defines the active vent field, but are not immediately adjacent to any active hydrothermal vents. Hole 858D was drilled by APC-XCB to 40.7 m, Hole 858G was rotary cored to 296.9 m, and Hole 858F was rotary cored from 276.5 m to 432.6 m. Both of

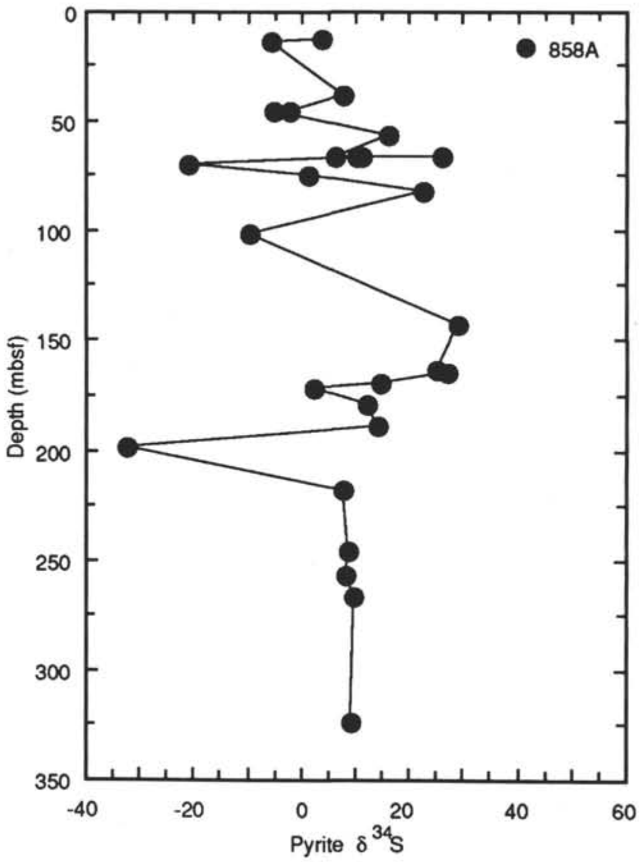

Figure 7. Sulfur isotope value of pyrite vs. depth for Hole 858A.

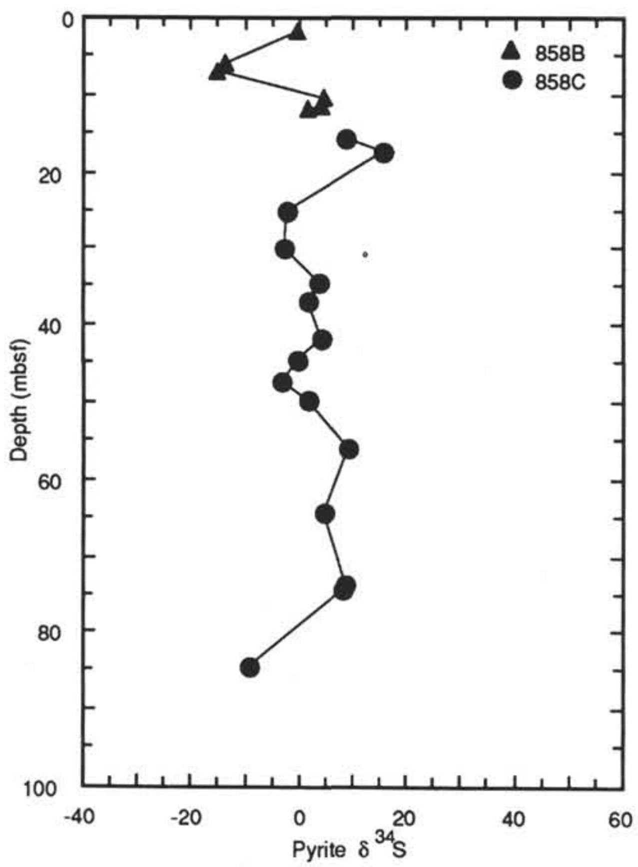

Figure 8. Sulfur isotope value of pyrite vs. depth for Holes 858B and 858C.

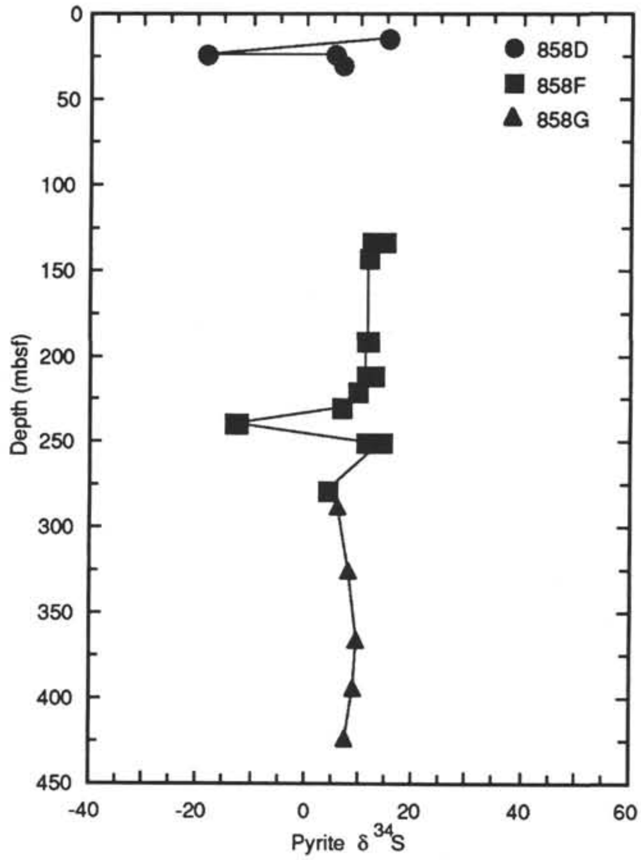

Figure 9. Sulfur isotope value of pyrite vs. depth for Holes 858D, 858F, and 858G.

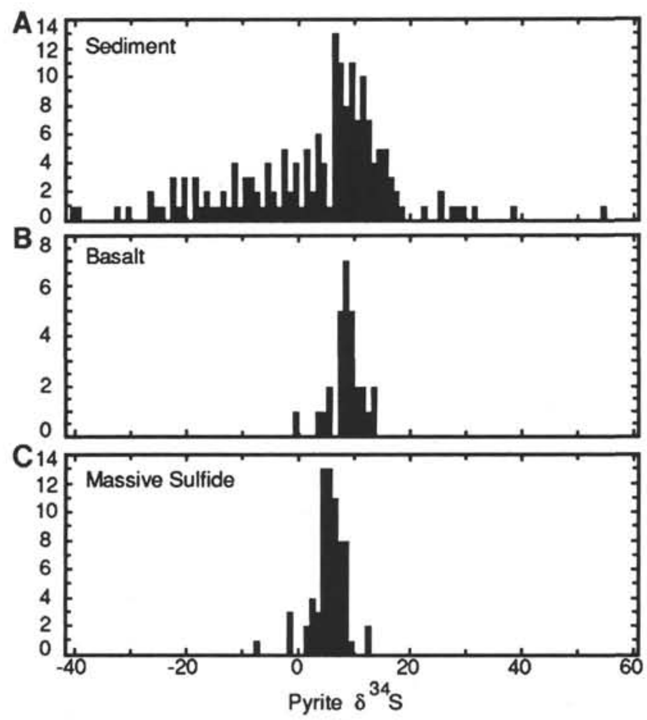

Figure 10. Histograms comparing the sulfur isotope values of pyrite in **(A)** sediment and metasedimentary rock, **(B)** basalt and diabase, and **(C)** massive, semimassive, and clastic sulfide.

the rotary cored holes had low core recovery. Basalt was recovered in Holes 858G and 858F below 249 mbsf. Pyrite in sediment from Hole 858D ranges in $\delta^{34}S$ from −18.7‰ to 15.1‰ (Fig. 9). Anhydrite has values of 23.2‰ and 23.5‰. The deeper sedimentary section sampled by Hole 858F contains pyrite with $\delta^{34}S$ values ranging from −13.2‰ to 14.7‰, but most samples have a narrow range, from 11‰ to 12‰ (Fig. 9). Two samples of anhydrite have $\delta^{34}S$ values slightly higher than seawater sulfate (22.1‰ and 23.4‰), but one sample has a low value of 11.4‰, similar to disseminated pyrite in the same sample (11.0‰). Pyrite in quartz-wairakite veins in basalt has $\delta^{34}S$ values of 13.3‰ and 13.8‰. Disseminated pyrite in basalt has a value of 4.0‰. All of the samples from Hole 858G are basalt or metabasalt. Pyrite disseminated in basalt has values of 7.3‰ to 9.7‰; pyrite in chlorite veins cutting basalt has values of 5.8‰ and 8.1‰ (Fig. 9). One sample of pyrrhotite in basalt has a value of 10.3‰. An anhydrite vein cutting basalt has a $\delta^{34}S$ value of 22.5‰, slightly higher than seawater sulfate.

SUMMARY OF DATA

Near-surface sediments generally have pyrite with isotopically light sulfur typical of diagenetic sulfide produced by sulfate-reducing bacteria. Some isotopically heavy pyrite with $\delta^{34}S$ values greater than seawater sulfate is present in the sediment, requiring high degrees of biogenic(?) reduction of sulfate. Earlier diagenetic pyrite formed in near-surface sediment is overprinted, either with depth or by proximity to the center of the hydrothermal field, by isotopically heavy (6‰ to 12‰) pyrite of hydrothermal origin. Anhydrite occurs in the hotter sections of the sediment pile that underlies the hydrothermal field and has isotopic values that tend to be several per mil higher than seawater sulfate, consistent with precipitation from recharging seawater that has undergone isotopic fractionation by preferential extraction of ^{32}S during sulfate reduction. Sulfide in altered igneous rocks is also isotopically heavy ($\delta^{34}S$ approximately 8‰; Fig. 10). Thus, primary basaltic sulfide (0.1‰, Sakai et al., 1984) is not the sole source of sulfur for the hydrothermal system; a heavier source of sulfur such as reduced seawater sulfate is required. Massive, semimassive, and clastic sulfides have a relatively narrow range of $\delta^{34}S$ values near 6‰, similar to hydrothermal sulfides in both sedimentary and basaltic rock that underlies the deposit.

ACKNOWLEDGMENTS

This study was supported by the Gilbert Research Fellowship Program of the U.S. Geological Survey, for which the author is deeply grateful. Doug White of the Water Resources Division of the U.S. Geological Survey in Menlo Park is thanked for access to and assistance with mass spectrometry.

REFERENCES*

Breit, G.N., Simmons, E.G., and Goldhaber, M.B., 1985. Dissolution of barite for the analysis of strontium isotopes and other chemical and isotopic variations using aqueous sodium carbonate. *Chem. Geol.,* 52:333–336.

Canfield, D.E., Raiswell, R., Westrich, J.T., Reaves, C.M., and Berner, R.A., 1986. The use of chromium reduction in the analysis of reduced inorganic sulfur in sediments and shale. *Chem. Geol.,* 54:149–155.

Davis, E.E., Mottl, M.J., Fisher, A.T., et al., 1992. *Proc. ODP, Init. Repts.,* 139: College Station, TX (Ocean Drilling Program).

Rees, C.E., 1978. Sulphur isotope measurements using SO_2 and SF_6. *Geochim. Cosmochim. Acta,* 42:383–389.

Rees, C.E., Jenkins, W.J., and Monster, J., 1978. The sulphur isotopic composition of ocean water sulphate. *Geochim. Cosmochim. Acta,* 42:377–381.

Sakai, H., Des Marais, D.J., Ueda, A., and Moore, J.G., 1984. Concentrations and isotope ratios of carbon, nitrogen and sulfur in ocean-floor basalts. *Geochim. Cosmochim. Acta,* 48:2433–2441.

* Abbreviations for names of organizations and publications in ODP reference lists follow the style given in *Chemical Abstracts Service Source Index* (published by American Chemical Society).

Date of initial receipt: 14 June 1993
Date of acceptance: 21 July 1993
Ms 139SR-226